Cell Reports, Volume *33*

Supplemental Information

Statistical Laws of Protein Motion in Neuronal Dendritic Trees

Fabio Sartori, Anne-Sophie Hafner, Ali Karimi, Andreas Nold, Yombe Fonkeu, Erin M. Schuman, and Tatjana Tchumatchenko

Supplemental Figures

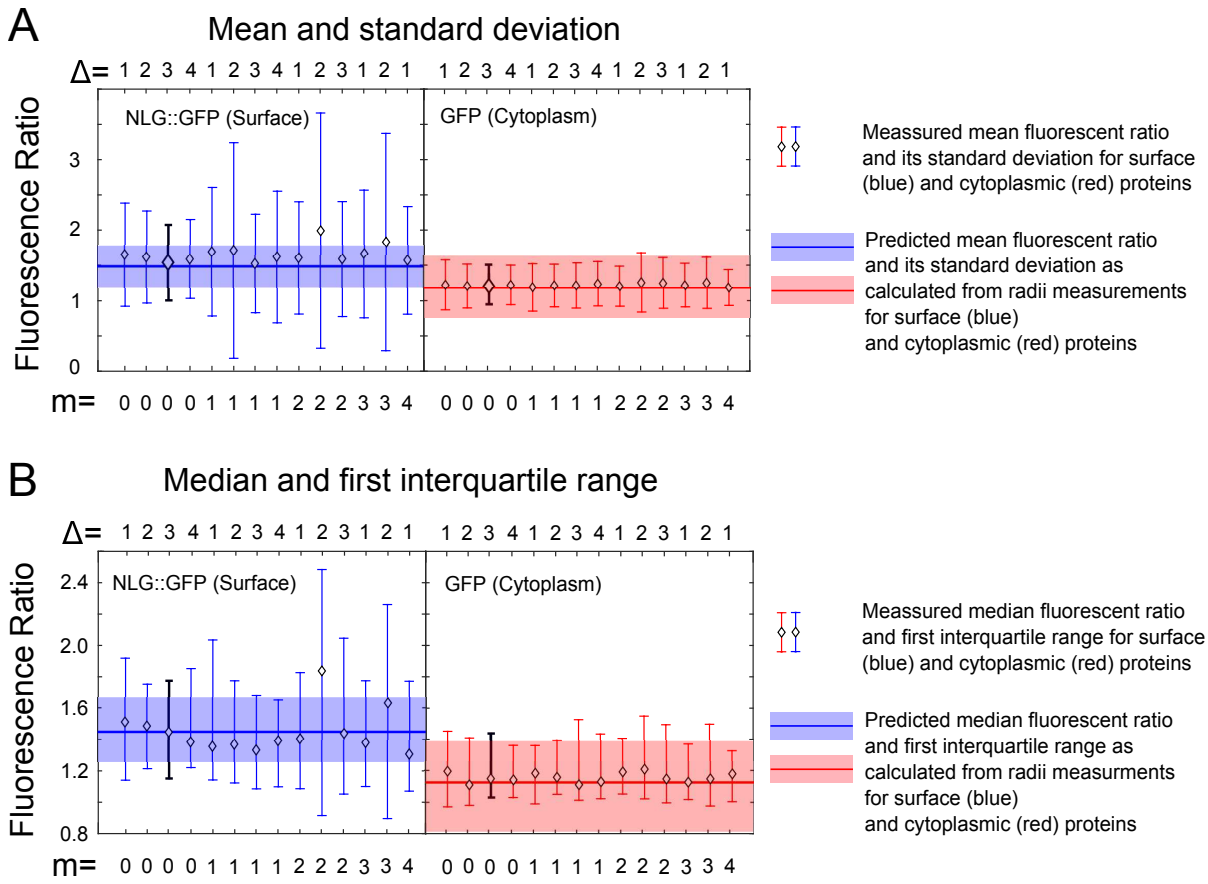

Figure S1: Supplemental data analysis related to Fig. 4 D. Two alternative calculations of error bars and averages associated with fluorescent signals and dendritic radii for surface and cytoplasmic proteins. (A) The error bar and center of each data point is calculated using the mean and standard deviation for GFP (cytoplasmic) and Nlg::GFP (surface) proteins, hereby Q_F^S (1.66, std= 0.99) and Q_F^C (1.26, std= 0.39). The predicted means and standard deviations of Q_P^S (1.48, std= 0.28) and Q_P^C (1.17, std= 0.43) that are calculated from dendritic radii ratios at branch points are shown as blue and red boxes. (B) The error bar and center of each data point is calculated using the median and interquartile range, hereby Q_F^S (1.41, IQR $1.1, 1.9$) and Q_F^C (1.18, IQR $1.01, 1.44$). The predicted medians and interquartile intervals of Q_P^S (1.45, IQR $1.27, 1.65$) and Q_P^C (1.12, IQR $0.84, 1.38$) that are calculated from dendritic radii ratios at branch points are shown as blue and red boxes.

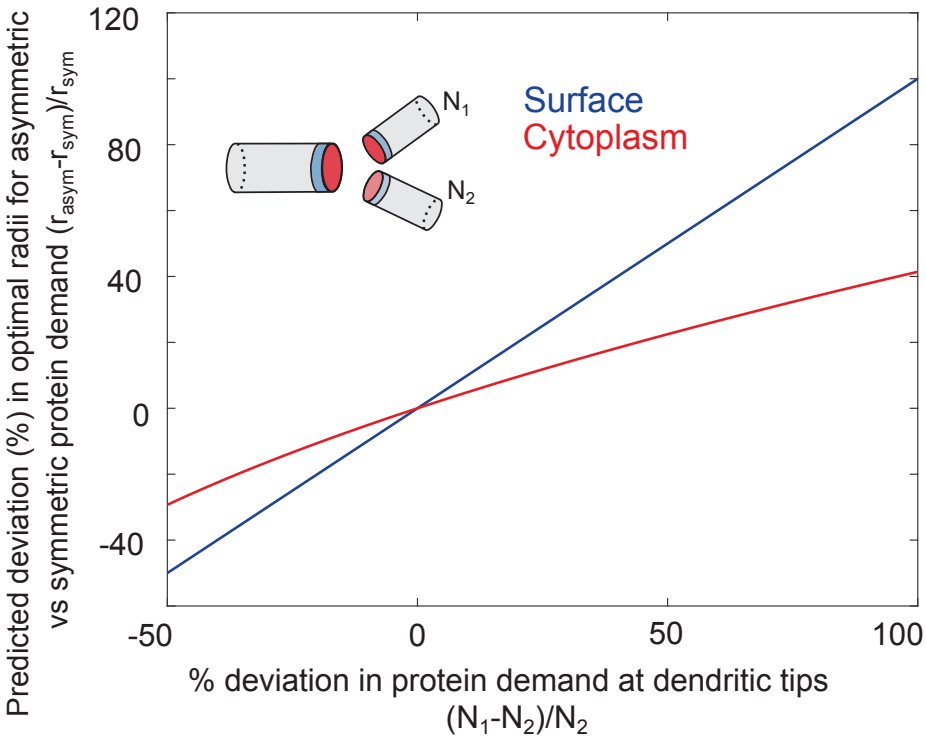

Figure S2: Supplemental analysis related to Fig. 5. Asymmetric protein demand and the associated optimal daughter radii. Synaptic plasticity can introduce asymmetric long-term protein demand downstream of a branch point (N_1 vs N_2). Here, we show how daughter radii that are optimal for the symmetric protein demand (shown in Fig. 5) deviate from those optimized for the asymmetric protein demand at the dendritic tips. Parameter choices as in Fig. 5.

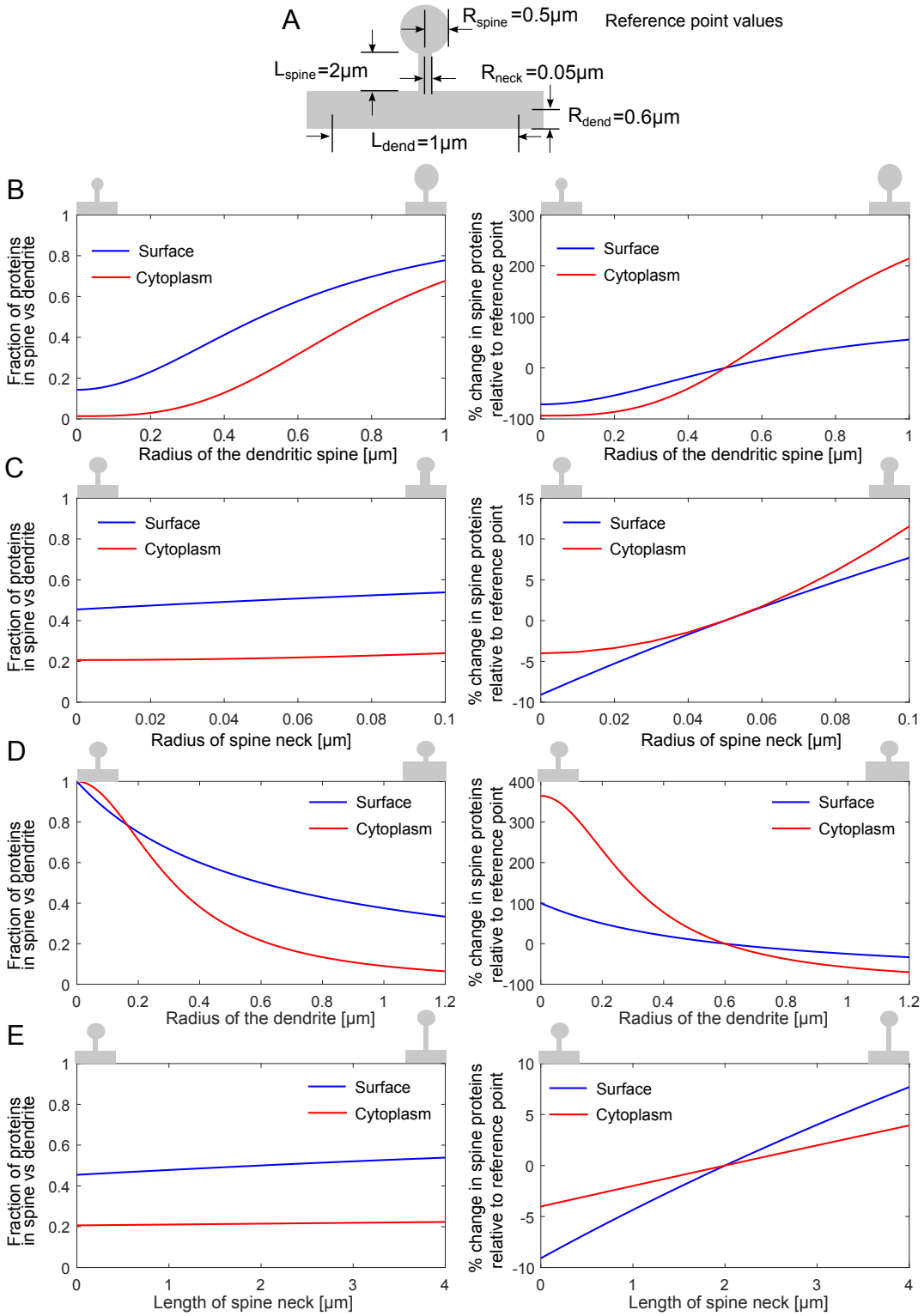

Figure S3: Supplemental figure related to Fig. 5. How does spine geometry shape the protein number in spines? To answer this question we assumed a constant protein density across the spine and dendrite and applied our branching calculations. (A) Spine geometry and default values used to exemplify the distribution of proteins in the spine and the local dendritic segment. Starting from this setting we varied each variable individually to investigate how it impacts the protein number in the spine. (B) Varying the radius of the spine head leads to a proportional increase in protein number. (C) Varying the radius of the spine neck has only a week influence on the protein number in a spine (D) Increasing the radius of the dendrite carrying the spine reduces the number of proteins in the spine. (E) Increasing the length of the spine neck does not significantly alter the protein number in the spine. On the left column we reported the absolute values of the fraction of proteins in spine, while on the right column we show the percentage variation of the fraction of protein in spines.

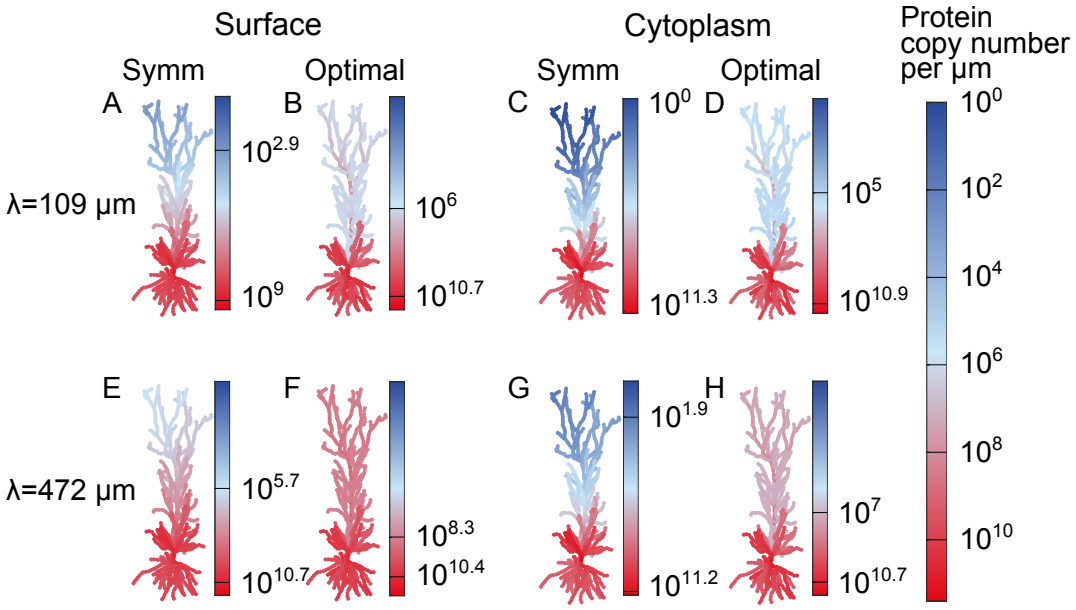

Figure S4: Supplemental analysis related to Fig. 6 C,D. Here, we show the predicted number of proteins per micrometer in a pyramidal neuron for different diffusion lengths for symmetrical and optimized branching radii for a protein with a different diffusion length $\lambda = 109\mu$m (top), this diffusion length corresponds to the median of the optimal diffusion lengths inferred from EM (Fig. 5C, blue) . As in Fig. 6 C,D the color code represents the predicted number of proteins per μm. We confirm that the number of proteins in the distal parts is larger for surface proteins than for cytoplasmic proteins with this diffusion length. As in Fig. 6, we considered symmetrical daughter branches where the radius of a daughter dendrite is $R_1 = R_2 = 0.75R_0$ and optimized daughter radii. In the bottom panels we show the distributions from Fig. C, D for comparison. Since we choose in the top panel a diffusion length that is smaller than that in Fig. 6 C,D the number of proteins that reach the dendritic tips is smaller than than in Fig. 6 C,D. To make sure that each compartment has at least one protein in the top and bottom panels we increase the number of proteins $2 \cdot 10^1 1$ in all panels of this figure to enable a quantitative comparison. The black horizontal lines on the color bars indicate the minimal and the maximal protein concentration in the respective figures.

Supplemental Table

λ (μm)	Protein Name	$\tau_{1/2}$ (days)	DOI	D ($\mu m^2/s$)	DOI	Method
686.9	Peroxiredoxin (half-life -3, diffusion -4)	7.3	10.7554/eLife.34202	0.52	10.1016/j.redox.2017.01.003	SER
450.7	Plexin-A	6.5	10.7554/eLife.34202	0.25	10.1016/j.bpj.2015.04.043	FC
97.4	Grm5 (Metabotropic glutamate receptor 5)	3.0	10.7554/eLife.34202	0.025	10.1523/JNEUROSCI.22-10-03910.2002	SPT
314.3	CamKII	7.2	10.7554/eLife.34202	0.111	10.1523/JNEUROSCI.4364-13.2014	SPT
75.5	Synaptophysin	9.2	10.7554/eLife.34202	0.005	10.3389/fnmol.2014.00091	FC
312.6	L1CAM (Neural cell adhesion molecule L1)	7.1	10.7554/eLife.34202	0.11	10.1083/jcb.200211011	SPT
104.2	Clathrin-L (b for half-life, c for Diffusion coeff.)	9.1	10.7554/eLife.34202	0.0096	10.3389/fnmol.2014.00091	FC
111.6	GluA1-AMPAR	2.0	10.1016/S0028-3908(98)00135-X	0.005	10.1093/brain/aws092	SPT
472.3	GABAAR subunit alpha 2	5.0	10.7554/eLife.34202	0.36	10.1093/brain/aws092	SPT
78.2	potassium channel Kv1.3	0.2	10.1016/j.neuroscience.2006.09.055	0.31	10.1093/brain/aws092	SPT
891.1	Syt7 (Synaptotagmin 7)	7.0	10.7554/eLife.34202	0.91	10.1021/bi5012223	SPT
73.4	Neurexin	3.6	10.7554/eLife.34202	0.012	10.1523/JNEUROSCI.4041-14.2015	SPT
168.3	AChE (acetylcholinesterase)	2.8	10.1111/j.1471-4159.1974.tb04319.x	0.08	10.1016/S0012-1606(89)80051-X	FRAP
344.6	VAMP2-pHluorin	6.8	10.7554/eLife.34202	0.14	10.1083/jcb.201604001	SPT
3360.5	Calbindin	4.5	10.7554/eLife.34202	20	10.1073/pnas.0407855102	FRAP
2137.6	GAP43(S41A) (Neuromodulin)	17.5	10.7554/eLife.34202	2.09	10.1091/mbc.e13-12-0737	FC
6162.8	Microtubule-Associated Protein Tau	101.6	10.7554/eLife.34202	3	10.1523/JNEUROSCI.0927-07.2007	FRAP
986.7	Phosphatidyl serine	22.0	10.1042/bj1600195	0.355	10.1091/mbc.e11-11-0936	FRAP & SPT
204	Actin	8.4	10.7554/eLife.34202	0.04	10.1073/pnas.1504762112	FRAP
4256.1	Rho-associated protein kinase 2	5.6	10.7554/eLife.34202	26	10.1038/ncomms10029	FC
103.1	GABA-A subunit $\alpha 1$	3.9	10.7554/eLife.34202	0.022	10.3389/fncel.2014.00151	SPT
302.4	GABA-A subunit $\alpha 5$	7.6	10.7554/eLife.34202	0.097	10.1038/ncomms7872	SPT
15	GluN2B	3.4	10.7554/eLife.34202	0.00053	10.1016/j.cell.2012.06.029	SPT
2110.7	Phosphoinositide phospholipase C	8.5	10.7554/eLife.34202	4.2	10.1101/521369	FC

λ (μm)	Protein Name	$\tau_{1/2}$ (days)	DOI	D ($\mu m^2/s$)	DOI	Method
3709.6	Glutamine synthetase	3.5	10.7554/eLife.34202	32	10.1023/A:1020574003027	QELS
582.7	Vesicle-associated membrane protein 2	6.8	10.7554/eLife.34202	0.4	10.1016/j.cell.2009.01.016	SPT

Table S1: Supplemental statistics of protein diffusion lengths related to Fig. 5. The first column of the table contains the protein diffusion length, the second column contains the name of the protein, the third and fourth contain the half life and the doi of the corresponding source. The fifth and sixth column contain the diffusion coefficient and the doi of the corresponding source. The last column is the technique used to measure the diffusion coefficient. SER stands for Stokes-Einstein Relationship, FC stands for Fluorescence Correlation, SPT stands for Single Particle Tracing and QELS for Quasi-elastic light scattering.